Size effect on quasi-brittle fracture

Xiaozhi Hu* and Kai Duan
School of Mechanical Engineering, University of Western Australia
35 Stirling Highway, Crawley, WA 6009, Australia

ABSTRACT

Size effect on fracture properties of MEMS and traditional materials is determined by the relative size of a testing specimen versus the material microstructure. In this study, size effect on quasi-brittle fracture is related to the length ratio determined by the fracture process zone (FPZ) and distance of a crack-tip to its nearest specimen boundary. It is shown that the tensile strength criterion applies if the specimen boundary is close to the crack-tip, and the fracture toughness criterion applies if the specimen boundary is away from the crack-tip. The specimen boundary influence reflects the dominant size effect mechanism, i.e. the interaction of the crack-tip FPZ with the specimen boundary. The boundary effect model proposed in the study is compared with the common size effect model emphasising exclusively the influence of specimen size, and the major difference is discussed.

Keywords: Size effect, boundary effect, quasi-brittle fracture, scaling, strength, fracture toughness

1. INTRODUCTION

Size effect on material properties and structure behaviour is relevant not only to nano-technology and nano-materials, but also traditional engineering materials. In the field of macro-mechanics, size effect is well-known for concrete specimens commonly measured from 100 mm to 5,000 mm in size. Although the absolute size of a concrete specimen is huge, the ratio of specimen size over the concrete structure (typically with the maximum aggregate size above 5 mm) is very similar to that of micro-specimens used for advanced material systems such as thin films and MEMS structures. For instance, micro-specimens of polysilicon measured from 2.5 to 7.5 μm in thickness and from 6 to 20 μm for the uncracked ligament have been used to determine the fracture toughness [1]. The average grain size of polysilicon is typically around 200 nm or larger. Those micro-polysilicon specimens and macro-concrete specimens have an almost identical specimen size and material structure ratio. The similar relative size ratio implies that those macro- and micro-specimens may face similar size effect issues besides their vast difference in absolute size. Because of the similarity, certain aspects of size effect dealt with by macro- fracture mechanics could provide valuable additions to the current nano-technology related size effect study, particularly in terms of fundamental size effect mechanisms.

Although the current study is confined mainly to macro- fracture mechanics, size effect issues relevant to micro-specimens can be addressed fundamentally in a similar way. Therefore, the current study emphasises the fundamental mechanism of size effect on quasi-brittle fracture, i.e. the physical origin of the apparent specimen size effect, based on the recent boundary effect model developed by the authors [2-5].

2. MODELLING OF QUASI-BRITTLE FRACTURE

Traditionally, size effect on quasi-brittle fracture of concrete-like engineering materials is described by the following relation [6]. The nominal strength σ_N of a specimen with an initial notch a is evaluated from the experimentally measured maximum load ignoring the present of the initial notch or crack, and is related to the specimen size W. The definition of σ_N is also illustrated in Figure 1.

* xhu@mech.uwa.edu.au; phone 61-8-6488 2812; fax 61-8-6488 1024; www.mech.uwa.edu.au/fracmech/

Third Intl. Conf. on Experimental Mechanics and Third Conf. of the Asian Committee on Experimental Mechanics, edited by Quan, Chau, Asundi, Wong, Lim, Proc. of SPIE Vol. 5852 (SPIE, Bellingham, WA, 2005) · 0277-786X/05/$15 · doi: 10.1117/12.621534

$$\sigma_N = \frac{A \cdot \sigma_T}{\sqrt{1+\frac{W}{W^*}}} \tag{1}$$

in which σ_T is the tensile strength, A and W^* are two empirical scaling parameters that need to be determined through curve-fitting to experimental measurements. There are two asymptotic limits for quasi-brittle fracture of concrete-like traditional engineering materials. The strength criterion σ_T is the dominant criterion for very small specimen size W while the fracture toughness criterion K_{IC} is the dominant criterion for very large W.

Equation (1) seems to suggest that the controlling parameter is specimen size W since the initial notch/crack a is not shown in the relation. It should be pointed out that a key condition for the applicability of equation (1) is that only geometrically similar specimens are considered by equation (1). That is specimens have the same geometry and have an identical initial notch (or crack) and specimen size ratio (a/W = α-ratio = constant). Under such a condition, specimen size W becomes the dominant parameter. However, one could argue the initial notch/crack length controls the observed size effect because α-ratio = constant and specimen size W can be replaced by crack a.

Clearly, the influence of the initial notch/crack has not been identified in equation (1). Furthermore, experimental evidence suggests that the scaling parameters A and W^* are α-ratio dependent, which suggests the initial crack length a has a strong influence on the observed size effect.

To emphasize the influence of the initial crack a and its relation with the specimen boundary, an idealised specimen condition, a large plate with a small edge crack (the geometry factor Y = 1.12), has been selected. It is assumed that the specimen size W is big enough so that it does not need to be considered. In this case, quasi-brittle fracture of the large plate is purely determined by the crack length a and is given by [7-9]:

$$\sigma_N = \frac{\sigma_T}{\sqrt{1+\frac{a}{a^*_\infty}}}$$

$$a^*_\infty = 0.25 \cdot \left(\frac{K_{IC}}{\sigma_T}\right)^2 \tag{2}$$

in which the reference a^*_∞ is a measurement of the crack-tip FPZ for a quasi-brittle material or the crack-tip plastic zone for a ductile material. Equation (2) has two well-defined asymptotic limits, σ_T and K_{IC}, for very short and very long cracks, respectively. The non-linear elastic fracture problems described by equation (2) can also be found in other material systems. For instance, the traditional elastic and plastic fracture of metals has the same asymptotic limits with σ_T and K_{IC} as the two extreme failure criteria.

The crack ratio, a/a^*_∞, in equation (2) describes the interactions between FPZ and its distance to the specimen front face boundary, which is also equal to the crack length in the case of an edge crack. The fracture transition from σ_T to K_{IC} described by equation (2) for W = constant is different to the size effect shown in equation (1) in which $W \neq$ constant.

Typical fracture mechanics specimens may not be treated as large plates. This is because the specimen back face boundary may also be fairly close to the crack-tip FPZ depending on the length of uncracked ligament (W-a). Also, the geometry factor, $Y = Y(\alpha) \neq 1.12$, varies with α-ratio. Equation (2) thus needs to be modified for a more general situation relevant to typical fracture mechanics specimens.

For a given material system, a specimen size W can always be found so that the condition of the linear elastic fracture mechanics (LEFM) is satisfied regardless whether $Y = 1.12$ or not. For instance, a concrete specimen with $W = 1$ m and α-ratio of 0.5. The nominal strength σ_N, which does not consider the presence of a crack, and fracture toughness K_{IC} are then related.

$$K_{IC} = \sigma_N \cdot Y(\alpha) \cdot \sqrt{\pi a} \tag{3}$$

For a finite-sized specimen, equation (3) is not valid if the α-ratio is close to 0 or 1, as the tensile strength σ_T becomes to dominate. The nominal strength σ_N, which does not consider the presence of a crack, is not an appropriate description of the stress state when the α-ratio is close to 1. To solve this problem, another nominal strength σ_n, which considers the presence of a crack, has been introduced [2-5] and is shown in Figure 1 together with σ_N. For the three-point-bending (3-p-b) situation, it can be found,

$$\begin{aligned} \sigma_N &= \mathrm{A}(\alpha) \cdot \sigma_n \\ \mathrm{A}(\alpha) &= (1-\alpha)^2 \end{aligned} \tag{4}$$

The $\mathrm{A}(\alpha)$ can also be easily determined for other specimen geometry such as compact tension or single-edge-notch-tension, following the definition shown in Figure 1.

Both σ_N and σ_n can be easily determined from the maximum load. If $\alpha \to 0$ (such as the case of a large plate), the two nominal strengths, σ_N and σ_n, are identical, and both should approach σ_T if the strength criterion is applicable. If $\alpha \to 1$, it is expected that the strength criterion σ_T should again be applicable, but only σ_n can be used to compare with σ_T as $\sigma_N \approx 0$. It is clear that to cover the entire α-ratio from 0 to 1, σ_n should be used instead of σ_N.

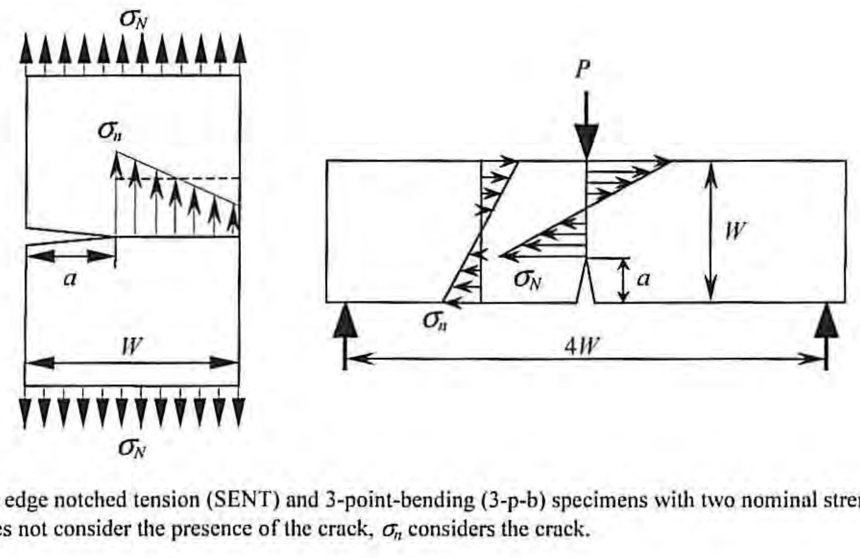

Figure 1. Single edge notched tension (SENT) and 3-point-bending (3-p-b) specimens with two nominal strengths: σ_N does not consider the presence of the crack, σ_n considers the crack.

The LEFM situation described by equation (3) can be taken as the asymptotic solution when the fracture toughness K_{IC} is valid, e.g. when the crack-tip is away from specimen boundaries. Since σ_n is identical to σ_N when $\alpha \to 0$, and is more suitable than σ_N as a strength measurement when $\alpha \to 1$, its variation with the crack length a is emphasised in this study.

σ_n can be solved from equations (3) and (4) following the recent work [2-5],

$$\sigma_n = \frac{K_{IC}}{\mathrm{A}(\alpha)\cdot Y(\alpha)\cdot\sqrt{\pi a}} = \frac{\sigma_T}{\sqrt{\dfrac{\left(\dfrac{\mathrm{A}(\alpha)\cdot Y(\alpha)}{1.12}\right)^2\cdot a}{\dfrac{1}{1.12^2\pi}\cdot\left(\dfrac{K_{IC}}{\sigma_T}\right)^2}}} = \frac{\sigma_T}{\sqrt{\dfrac{a_e}{a_\infty^*}}} \tag{5}$$

The equivalent crack a_e is introduced in equation (5) so that it has form of equation (5), which is given by:

$$a_e = \left(\frac{A(\alpha)\cdot Y(\alpha)}{1.12}\right)^2\cdot a \tag{6}$$

Equation (2) is identical to the K_{IC} criterion if $a/a^*_\infty >> 1$, which becomes:

$$\sigma_N = \frac{\sigma_T}{\sqrt{\dfrac{a}{a_\infty^*}}} \tag{7}$$

Comparing equations (5) and (7), the general asymptotic solution for small specimens can be written as follows [2-5]:

$$\sigma_n = \frac{\sigma_T}{\sqrt{1+\dfrac{a_e}{a_\infty^*}}} \tag{8}$$

Different to equations (3), (5) and (7) that are valid under the LEFM condition, equation (8) covers the entire fracture range from the strength criterion σ_T to K_{IC} criterion including the quasi-brittle fracture region between the two fracture criteria.

Different to equation (1), which is applicable only to geometrically similar specimens, equation (8) can be used to analyse experimental results from any fracture mechanics specimens, e.g. same size but different α-ratios, and even different geometries. This is because the geometry influence has been considered by the α-ratio-containing equivalent crack a_e. The physical meanings of the two scaling parameters are also clear, σ_T is the tensile strength, a^*_∞ is the measurement of the crack-tip FPZ, and both are material constants. Of course, equation (8) is also applicable to geometrically similar specimens with a constant α-ratio. In this case, equation (1) can be derived from equation (8) as a special case for α-ratio = constant. The two scaling parameters are given by:

$$A = A(\alpha)$$

$$W^* = W\cdot\frac{a_\infty^*}{a_e} = \frac{a_\infty^*}{\alpha\cdot\left(\dfrac{A(\alpha)\cdot Y(\alpha)}{1.12}\right)^2} \tag{9}$$

It is clear both A and W^* are α-ratio dependent. Without equation (9), they remain empirical scaling parameters, and have to be determined from experimental data through curve-fitting. Furthermore, separate curve-fitting processes are required to determine A and W^* for different geometrically similar specimens (e.g. even if only the α-ratio is changed).

It is worthwhile pointing out again that equations (2) and (8) are derived through considering the specimen boundary influence and interactions between FPZ and specimen boundaries. Specimen size W is not considered as the dominant factor on the apparent "size effect". It is interesting to see the traditional size effect relation as given by equation (1) has been derived from the boundary effect model. Therefore, the dominant size effect mechanism is actually the interaction between FPZ and specimen boundary, or boundary effect.

Rearranging equations (8) and (1), following linear relations suitable for curve-fitting can be established.

$$\frac{1}{\sigma_n^2} = \frac{1}{\sigma_T^2} + \frac{1}{\sigma_T^2} \cdot \frac{a_e}{a_\infty^*} \tag{10}$$

and

$$\frac{1}{\sigma_N^2} = \frac{1}{(A\sigma_T)^2} + \frac{1}{(A\sigma_T)^2} \cdot \frac{W}{W^*} \tag{11}$$

The two scaling parameters in equations (1) or (8) can be easily determined from experimental results using the above linear relations.

If material constants σ_T and K_{IC} are known, curve-fitting is not required for the boundary effect model, equation (8). Quasi-brittle fracture behaviour can be predicted directly from known σ_T and K_{IC}. Alternatively, important material properties σ_T and K_{IC} can now be determined from quasi-brittle fracture results as shown in equation (10). However, curve-fitting is always necessary for the size effect relation, equation (1), unless the detailed expressions such as those given by the boundary effect model, equation (9), are used.

3. ANALYSIS OF EXPERIMENTAL RESULTS

Two different sets of experimental results measured from geometrically similar and dissimilar specimens are selected to illustrate the applications of the boundary effect model, equation (8). The results from geometrically dissimilar 3-p-b specimens [10] are shown in Figure 2. The span-to-depth ratio is 5. The nominal strength σ_n results of all specimens approach that of the smallest specimen ($W = 5$ mm) when $\alpha \to 0$ or 1, which provides a reliable estimation of the tensile strength $\sigma_T = 10.29$ MPa. If the nominal strength σ_N is used, the asymptotic limit at $\alpha \to 1$does not equal to σ_T.

The traditional size effect model, equation (1), requires geometrically similar specimens, or a constant α-ratio. Therefore, the results in Figure 2 cannot be analysed by equation (1). However, the present boundary effect model, equation (8), does not require such a condition.

The results in Figure 2 are replotted in Figure 3 following the forms of equations (10) and (11). The tensile strength σ_T and fracture toughness K_{IC} (through the reference crack a^*_∞) are determined from Figure 3(a) using equation (10). However, the nominal strength σ_N data in Figure 3(b) cannot be analysed by equation (11) because the 3-p-b specimens are not geometrically similar. Therefore, the size effect model, equation (1), cannot explain the results. The straight lines in Figure 3(b) for different α-ratios are the predictions from the boundary effect model, equation (8), based on the results in Figure 3(a).

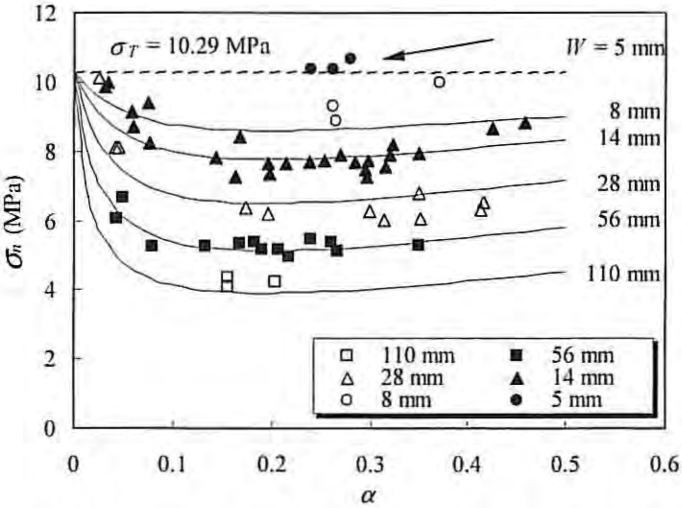

Figure 2. Comparisons of experimental results [10] with predictions from the boundary effect model.

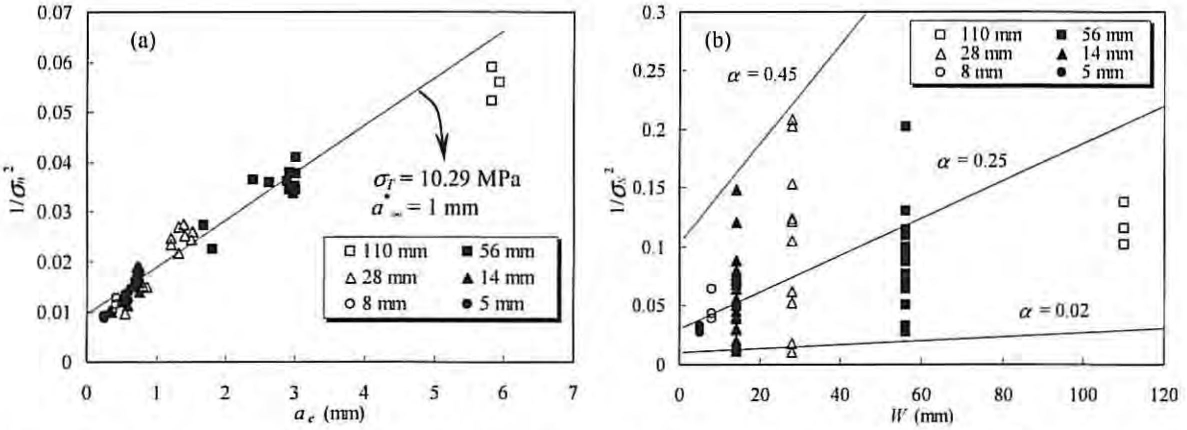

Figure 3. (a) Determination of material constants σ_T and a^*_∞, and (b) predictions from the from the boundary effect model.

The predicted strength and toughness controlled fracture regions together with the transitional quasi-brittle fracture region for the most commonly used 3-p-b geometry with the span-to-depth ratio of 4 are shown in Figure 4. The crack ratio, a_e/a^*_∞, as used in equation (8) provide a convenient measurement for those different fracture regions. It is clear from Figure 4 that even very large specimens (e.g. $W/a^*_\infty > 1{,}000$) can still experience quasi-brittle fracture or even strength controlled failure if the α-ratio is very small or close to unity, which shows the specimen boundary indeed influences the material fracture behaviour. To our best knowledge, a clear fracture map on various fracture regions as given in Figure 4 has not been shown before by the size effect model.

The nominal strengths of a high strength concrete from three groups of geometrically similar 3-p-b specimens with three different α-ratios [11] are shown in Figure 5. The span-to-depth ratio is 4 for those specimens. The boundary effect relation shown in Figure 5 (a) is unique while three linear relations exist for the size effect solution depending on the α-

ratio as shown in Figure 5(b). The results in Figure 5 further demonstrate the boundary effect model, equation (8), has much wider applications than the traditional size effect model, equation (1).

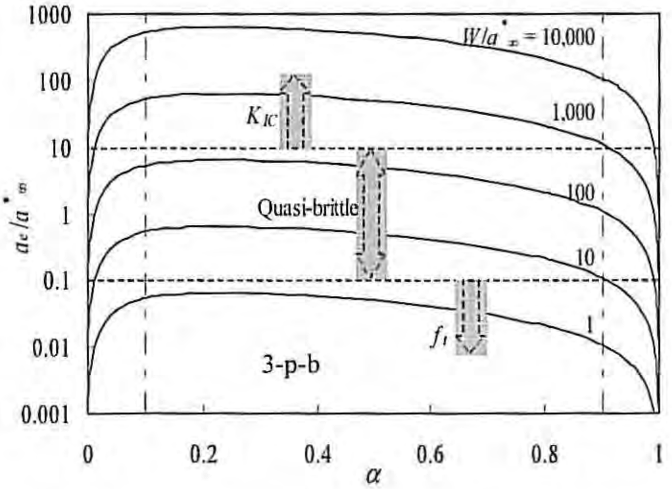

Figure 4. Fracture transition zones of 3-p-b specimens showing the influence of specimen size and boundaries.

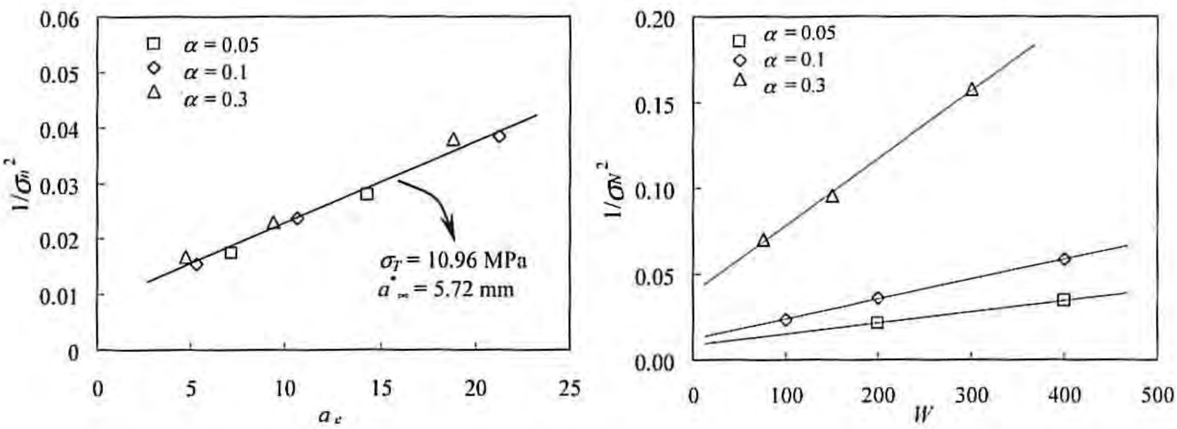

Figure 5. (a) Unique linear relation from Eq (10), and (b) three different linear relations from Eq (11).

4. DISCUSSION AND CONCLUSIONS

Contrary to the common belief that size effect on fracture properties is induced by the variation of specimen size W, the present study based on consideration of the specimen boundary influence shows that the relative crack ratio, a_e/a^*_∞, scaled by FPZ controls the size effect. That is the reason why micro-specimens of MEMS materials with FPZ comparable to the size of micro-specimens would show similar size effect as those macro-specimens of traditional quasi-brittle materials. The size effect issue certainly needs to be addressed when interpreting experimental results and studying fracture initiated from micro-cracks. It has been reported that the fracture toughness of polysilicon measured from micro-specimens could vary from 1.6 to over 3.2 MPa√m [1] even after excluding a group of results show extra-ordinary high fracture toughness values. Clearly, a wrong selection of the fracture toughness value would lead a huge error in the estimation of micro-cracks.

The experimental results examined in the present study clearly show that the traditional size effect model, equation (1), is inadequate, as it can only be used for a single set of geometrically similar specimens. As a matter of fact, equation (1) is only a special case of the present boundary effect model, equation (8). Applications of equation (8) are much more flexible. Most importantly, the present boundary effect model addresses the fundamental mechanisms of size effect, i.e. the influence of specimen boundary on fracture and the interaction of specimen boundary with FPZ.

The reference crack a^*_∞ as a measurement of crack-tip FPZ is an important material property. As shown in Figure 4, the equivalent crack a_e scaled by a^*_∞ has effectively combined contributions from both the front and back face boundaries together. Such a clear definition of various fracture regions has not been reported before in the literature.

ACKNOWLEDGEMENT

The financial support from the Australian Research Council (ARC) through a Discovery Projects grant is acknowledged.

REFERENCES

1. R. Ballarini, R.L. Mullen, Y. Yin, H. Kahn, S. Stemmer, and A.H. Heuer, The fracture toughness of polycrystalline silicon microdevices: A first report, *J. Mater. Res.* **12** [1], 915-922(1997).
2. K. Duan and X.Z. Hu, Specimen boundary induced size effect on quasi-brittle fracture, *Strength, Fracture and Complexity* **2**, in press (2004).
3. K. Duan, X.Z. Hu and F.H. Wittmann, Scaling of quasi-brittle fracture: boundary and size effect, *Mater. Mech.*, in press (2004).
4. K. Duan and X.Z. Hu, Asymptotic analysis of boundary-effect on strength of concrete, in: V.C. Li, C.K.Y. Leung, K.J. Willam, S.L. Billington (Eds.), *Fracture Mechanics of Concrete Structures (Proc. FraMCoS-5)*, Ia-FraMCoS, Vol.1, pp.197-204 (2004).
5. K. Duan and X.Z. Hu, Asymptotic analysis of boundary effect on fracture properties of notched bending specimens of concrete, in: A.V. Dyskin, X.Z. Hu, E. Sahouryeh (Eds.), *Structural Integrity and Fracture* (*Proc. SIF2002*), eds., A.A.Balkema Publishers, Lisse, The Netherlands, pp.19-24 (2002).
6. Z.P. Bažant, Size effect in blunt fracture: concrete, rock, metal, *J. Eng. Mech. (ASCE)* **110**, 518-535(1984).
7. X.Z. Hu, Size effect in toughness induced by crack close to free edge, in: H. Mihashi, K. Rokugo (Eds.), *Fracture Mechanics of Concrete Structures* (*Proc. FraMCoS--3*), Aedificatio Publishers, Freiburg, pp.2011-2020 (1998).
8. X.Z. Hu, An asymptotic approach to size effect on fracture toughness and fracture energy of composites, *Eng. Fract. Mech.* **69**, 555-564 (2002).
9. X.Z. Hu, and F.H. Wittmann, Size effect on toughness induced by crack close to free surface, *Eng. Fract. Mech.* **65**, 209-221 (2000).
10. D.D. Higgins, and J.E. Bailey, Fracture measurements on cement paste, *J. Mater. Sci.* **11**, 1995-2003 (1976).
11. B.L. Karihaloo, H.M. Abdalla and Q.Z. Xiao, Size effect in concrete beams, *Eng. Fract Mech.* **70**, 979-993 (2003).